



ELSEVIER

Biochimica et Biophysica Acta 1537 (2001) 110–116



www.bba-direct.com

Fluidity of the myelin sheath in the peripheral nerves of diabetic rats

Marta Zuvic-Butorac ^{a,*}, Jasna Kriz ^{b,1}, Ante Simonic ^b, Milan Schara ^c

^a Department of Physics, Faculty of Medicine, University of Rijeka, B. Branchetta 20, 51000 Rijeka, Croatia

^b Department of Pharmacology, Faculty of Medicine, University of Rijeka, B. Branchetta 20, 51000 Rijeka, Croatia

^c Institute 'J. Stefan', University of Ljubljana, Jamova 39, 1000 Ljubljana, Slovenia

Received 8 January 2001; received in revised form 29 May 2001; accepted 30 May 2001

Abstract

In the present study we examined the structural integrity of the myelin sheath in the peripheral nerves from short-term streptozotocin (STZ)-treated diabetic rats, using ESR spectroscopy as a tool in determining the dynamic state and the structure of the myelin lipid phase. Experiments were performed on spin-labeled sciatic and sural nerves from STZ-treated Hannover–Wistar rats and age-matched controls. The spectrum analysis employed a numerical simulation model with the set of fitting parameters that in the same time relate the ESR line shape and structure and dynamics of the probed environment. The simulation considered three spectral components weighted and summed in the composite spectrum. The comparative analysis of results showed the fraction of the spectral component II to be significantly increased in the spectra of diabetic rats, indicating the significant increase in overall fluidity of the myelin structure. The origin of fluidity changes was further investigated using an experimental model for demyelination (local injection of ethidium bromide *in vivo*), proteolytic action of trypsin *in vitro*, and osmotic myelin swelling *in vitro*. Analysis and comparison of the results suggested a conclusion in terms of changed biophysical properties of the myelin lipid phase in peripheral nerves in the pathology of diabetes. © 2001 Elsevier Science B.V. All rights reserved.

Keywords: Myelin sheath; Peripheral nerve; Streptozotocin-induced diabetes; Rat; Electron spin resonance; Lipid phase fluidity

1. Introduction

The peripheral neuropathy associated with diabetes is one of the most common polyneuropathies and at least 50% of diabetic patients will develop a form

of diabetic neuropathy within 25 years after diagnosis. The characteristic histopathological findings are axonal degeneration, secondary myelin break-down resulting in so-called secondary demyelination and atrophy. The underlying pathological mechanisms are unclear. However, possible factors involved are protein glycosylation, accumulation of polyols, altered lipid metabolism, decreased myo-inositol content, altered Schwann cell function, local ischemia and lack of neurotrophic factors [1–3].

Although, as a general phenomenon, segmental and paranodal demyelination is the feature of long-term diabetic neuropathy, some ultrastructural changes of the myelin sheath in early diabetes must

Abbreviations: STZ, streptozotocin; ESR, electron spin resonance; EB, ethidium bromide

* Corresponding author. Fax: +385-51-651-177.

E-mail address: martaz@mamed.medri.hr (M. Zuvic-Butorac).

¹ Present address: Center for Research in Neurosciences, McGill University, The Montreal General Hospital Research Institute, Montreal, QC, Canada H3G 1A4

not be excluded. Morphological findings in diabetic neuropathy are associated with widespread disturbances of axonal membrane excitability and consequently peripheral nerve dysfunction [2–4]. An early feature of diabetic nerve damage in humans is reduction of sensory and motor nerve conduction velocity accompanied by abnormalities in compound nerve action potentials later associated with progressive nerve fiber loss, atrophy and concomitant deterioration of neural function [4]. Our electrophysiological studies performed on the peripheral nerves of short-term streptozotocin (STZ)-diabetic rats, used as a model of early diabetes, revealed significant reduction in nerve conduction velocity associated with selective defects in the function of the inward rectifier – specifically internodal, predominantly potassium conductance that regulates nerve excitability [5,6]. Similar functional defects are recently described in humans [7], suggesting that beside probable structural changes of ion channels (glycosylation, phosphorylation), some additional ultrastructural changes in myelin structure might occur prior to chronic demyelination, possibly being an early event associated with the development of diabetic neuropathy.

In the present study we examined myelin sheaths in the peripheral nerves from short-term streptozotocin (STZ)-diabetic rats using electron spin resonance (ESR) spectroscopy as a tool in determining changes of myelin lipid phase ordering and dynamics. To assess possible explanations for the changes of fluidity, we applied a frequently used experimental model for demyelination (local treatment with ethidium bromide (EB) *in vivo*), as well as two simple models for membrane fluidization (proteolytic action of trypsin and osmotic stress *in vitro*). Both models were analyzed using the same methodology of ESR on the spin-labeled myelin lipid phase.

2. Materials and methods

2.1. Experimental models

Experiments were performed on STZ-treated Hannover–Wistar male rats and age-matched controls. Diabetes was induced in 3–4-weeks-old rats (weight 90–100 g) by three consecutive injections of STZ (45 mg/kg *i.p.* 3 days in the row). The rats were

weighed regularly and blood glucose levels were measured (Glucometer ELITE 3904M, Bayer) in samples drawn from the tail vein. After 12 weeks of diabetes animals showed marked hyperglycemia, 24.21 ± 0.98 mmol/l vs. 8.28 ± 0.66 mmol/l (mean \pm S.E.M., $n=10$) with an approximate weight loss of 30% in diabetic animals.

Diabetic animals were killed by overdose of anesthetic. Sciatic and sural nerves of approximately 2 cm length were quickly dissected out from each rat, pinned to the bottom of the wax-coated chamber and carefully desheathed. Isolated nerves were continuously perfused with mammalian Ringer's solution containing in mmol/l: 127 NaCl, 1.9 KCl, 2.4 CaCl₂, 1.2 KH₂PO₄, 1.3 MgSO₄, 26 NaHCO₃ and 10 glucose. After the surgical procedure was finished, the nerves were gently put into the testing capillary tube for spin labeling.

The experiments with induced demyelination were performed on the age-matched healthy animals, with local injection of 1% EB in the surgically opened right-hand side sciatic nerve. The left-hand side sciatic nerve served as the control. After 7 days the animals were sacrificed, and the procedure of dissection and preparation for spin labeling was the same as described previously.

The experiments with model fluidization by trypsin were done on dissected and isolated sciatic nerves from healthy animals. Desheathed nerves were kept in trypsin solution (625 mg trypsin/500 ml) for 1 h at 40°C, washed and returned to Ringer's solution for spin labeling afterwards.

In the experiments with changed osmotic conditions, already prepared sciatic nerves were put into hypo-osmolar (210 mmol/l) or hyper-osmolar (350 mmol/l) Ringer's solution (osmolarity adjusted by decreased or increased NaCl content).

2.2. Spin labeling

The prepared nerve sample was incubated (5 min) with 6×10^{16} molecules of lipophilic spin probe, methyl ester of 5-doxyl palmitate MeFASL(10,3) (synthesized by Prof. S. Pečar, Faculty of Pharmacy, University of Ljubljana, Slovenia), uniformly distributed over the walls of the glass tube. The labeled sample was transferred into a glass capillary (1 mm inner diameter) and the ESR spectrum immediately

recorded on a Bruker 300 spectrometer ($P = 10$ mW, $f = 9.3$ GHz), at 37°C .

2.3. ESR line shape evaluation

The ESR spectrum of lipid spin probe incorporated in the lipid bilayer can be calculated using the spin Hamiltonian, in which the organization and dynamics of neighboring molecules are considered to partially average the components of the interaction tensors. The formalism for the calculation of the spectrum was performed according to the model developed by Schindler and Seelig [8]. This model provides a set of fitting parameters that in the same time relate to the ESR line shape and reflect the structure and dynamics of the probed environment. Using the appropriate set of parameters, one can produce an ESR spectrum $s(B)$ (B -magnetic field):

$$s(B) = s(S_1, S_3, \tau_{20}, \tau_{22}, B) \quad (1)$$

The order parameters S_3 and S_1 describe the average amplitude of motion (or time-averaged position) of the long molecular axis of the nitrogen $2p\pi$ orbital, relative to the bilayer normal and perpendicular to the bilayer normal, respectively, while rotational correlation times τ_{22} and τ_{20} refer to the rotation around and perpendicular to the long molecular axis of the spin label, respectively.

In applying the model to the analysis of the complex myelin sheath spectra, we found that a reasonably good fit could be obtained employing three typical spectral components $s_i(B)$, calculated using Eq. 1, weighted and summed in the composite spectrum $S(B)$.

$$S(B) = \sum w_i s_i(B) \quad (2)$$

$$\sum w_i = 1 \quad (3)$$

The weighting factor w_i of a component $s_i(B)$ represents its relative contribution to the whole spectrum. The weighting factors of the spectral components in the composite calculated spectrum (that is to fit the experimental one), could be computed by the linear least squares approach in which the optimal values of w_i are evaluated through the maximum likelihood

of the least squares merit function. The goodness of fit was deduced from the χ^2 -value.

3. Results

3.1. ESR spectra of myelin sheath lipid phase

The lipophilic spin probe MeFASL(10,3) incorporated into the lipid rich myelin sheath of prepared nerve samples obtained from SZT-induced diabetic rats as well as control animals, enabled us to record the respective ESR spectra. The spectra were stable, indicating that there was no reduction of the NO moiety to the EPR silent form that could have taken place if the probes penetrated into the interior of the axons. On the other hand, the amount of spin probe used for labeling was calculated for the average total lipid content of the myelin sheath, and since spectra showed no spin exchange broadening, we assumed that the signal obtained was predominantly from the myelin sheath labeled evenly throughout.

Since the myelin sheath is structured as a multi-layered membrane bilayer of the Schwann cell, the recorded spectra were analyzed by a simulation

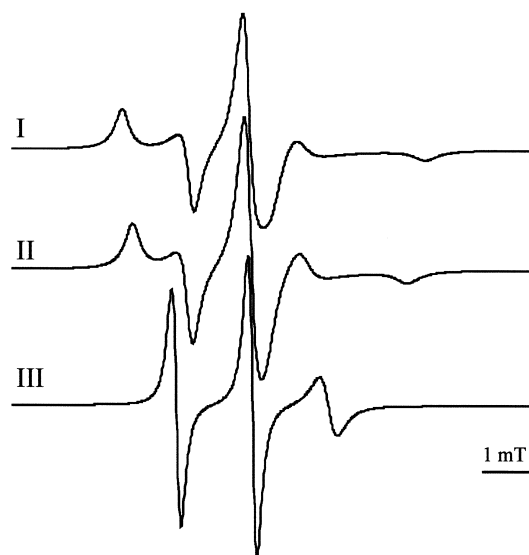


Fig. 1. Spectral components calculated by Eq. 1, used in simulation of experimental spectra of spin probe MeFASL(10,3) incorporated into the myelin sheath lipid phase of peripheral nerves. The components were chosen in order to meet some empirical and numerical requirements explained in Section 3. The numerical parameters for calculation of each component are listed in Table 1.

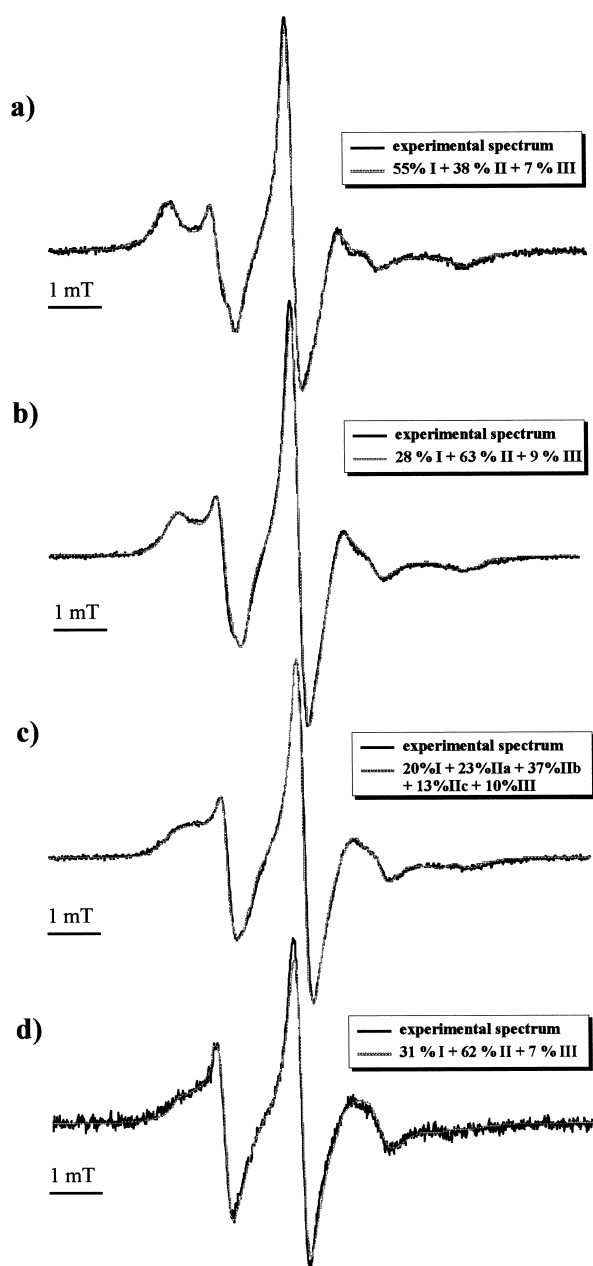


Fig. 2. Experimental and simulated ESR spectra of spin probe MeFASL(10,3) incorporated into the myelin sheath lipid phase of peripheral nerves. All spectra were taken at 37°C. Weighting factors (expressed as percentage) of the components are indicated. (a) control spectrum, (b) spectrum taken from sciatic nerve of diabetic rat (c) spectrum taken from sciatic nerve of the animal that developed strong diabetic symptoms. The simulation had to be performed employing five spectral components with order parameters S_3 of 0.64, 0.52, 0.38, 0.3 and 0.05 with rotational correlation times τ_{20} in the range of 1.2 to 0.8 ns. (d) spectrum of EB-treated nerve.

method developed for lipid bilayers. The recorded spectral line shapes reflect the microenvironment structure and dynamics of the myelin sheath; therefore, the parameters used in simulation analysis allowed us to estimate the fluidity of the probed myelin structure.

According to the results of other authors obtained on the model membranes [9,10] and our previous results on biomembranes [11], the reasonable fitting of ESR spectra at 37°C could be made using three spectral components. The choice of the spectral components for our fitting procedure was made as follows: the parameters for the most ordered component (I) were obtained by adjusting the outer hyperfine splitting in control sample spectra, while the parameters for the most fluid component (III) were taken from the simulation of the inner hyperfine splitting of the homogenized control samples' spectra. The fitting parameters for intermediate spectral component (II) were deduced from the minimization of the χ^2 -value in the control spectra. Once the components were defined (Fig. 1), the parameters were kept constant (Table 1), and weighting factors changed in order to produce the best possible fit in terms of the minimal χ^2 -value.

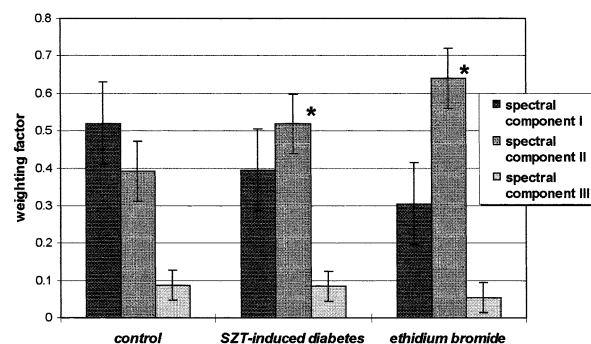


Fig. 3. Weighting factors for spectral components obtained in the simulation of experimental spectra of spin probe MeFASL(10,3) incorporated into the myelin sheath lipid phase of peripheral nerves. Weighting factors of spectral components directly relate to the proportion of the spin-labeled molecules that are probing structurally and dynamically different environments in the myelin sheath. Presented are the mean values \pm S.E.M. with the number of samples as follows: $N(\text{control})=12$, $N(\text{SZT-induced diabetes})=20$, $N(\text{EB})=5$. Spectra were taken at 37°C. Statistical significance for the comparison to the control value is indicated by $*(P < 0,05)$.

Table 1

The parameters for spectral components used in simulation of experimental spectra of spin probe MeFASL (10,3) incorporated in the myelin sheath lipid phase of peripheral nerves

Spectral components	Order parameters		Rot. corr. times (ns)	
	S_3	S_1	τ_{20}	τ_{22}
I	0.62	-0.3	1.4	3
II	0.50–0.54	-0.2	1.2	2
III	0.05–0.1	0	0.6–0.8	0.6–0.8

The parameters listed were the same for spectra obtained from control animals, rats with SZT-induced diabetes, and EB-treated nerves.

3.2. ESR spectra of diabetic animals' myelin sheath

The values of weighting factors did not differ significantly for the samples obtained from the same animal, not within the control, nor within the diabetic group. However, the weighting factors of the component II in the spectra of samples from diabetic rats had significantly elevated values in comparison to the corresponding controls (Figs. 2 and 3). This result suggests an increase in the number of the molecules that sensed less restricted movement, and therefore indicates an increase in the overall fluidity of the myelin sheath. Interestingly, the samples taken from two animals that had had very pronounced diabetic symptoms, appeared all to have spectral component II 'split' in the whole range of components of gradually diminishing order and dynamic parameters, indicating a decrease in overall order of the myelin sheath lipid phase (Fig. 2c).

3.3. ESR spectra of EB-treated myelin sheath

ESR spectra of EB-treated sciatic nerves showed qualitatively the same kind of change as did the

nerves isolated from diabetic animals (Fig. 2). Namely, the spectra could be fitted with the same three components as controls (with the notion that these controls were not altered with respect to other control spectra), but with increased weight of spectral component II (Table 2).

3.4. ESR spectra of trypsin-treated myelin sheath

In vitro trypsin-treated sciatic nerves showed markedly another type of fluidity change. The spectra could not be satisfactorily fitted by the components used in spectral analysis of control spectra, as long as the order parameters were not significantly decreased: in spectral component I for 10%, and in spectral component II for 33% (Table 2).

Additionally, the weight of component III had to be increased (for 25%) in order to produce a reasonably good fit. This type of fluidity change suggests a significant decrease of order in the myelin sheath under the proteolytic action of trypsin, which is another type of change compared to one produced by EB.

3.5. ESR spectra of myelin sheath under changed osmotic conditions

Although one can expect the change of lipid phase ordering and dynamics under changed osmotic conditions, by the method applied we could not detect any difference with respect to control spectra, either in hypo-osmotic nor in hyper-osmotic conditions.

Table 2

Spectral parameters used in simulation of experimental spectra obtained on trypsin-treated samples

Spectral components	Order parameters		Rot. corr. times (ns)		Weighting factors
	S_3	S_1	τ_{20}	τ_{22}	
I	0.56	-0.2	1.4	5	0.50 ± 0.08
II	0.36	-0.15	1.2	5	0.31 ± 0.03
III	0.05	0	0.8	0.8	0.18 ± 0.08

Weighting factors for spectral components are presented as mean values \pm S.E.M. for 11 spectra. Spectra were taken at 37°C.

4. Discussion

In this work we applied ESR spectroscopy to the

spin-labeled myelin sheath lipid phase in order to at least partially answer frequent questions on subtle changes of myelin structure in the pathology of peripheral neuropathy in diabetes [12]. As a model we chose peripheral nerves of rats with SZT-induced diabetes [13], in which the peripheral neuropathy is still questioned [14], although it develops early functional and biochemical defects but with very mild (or no) morphological changes in the peripheral nerves [15–17].

The method of ESR with a lipophilic spin probe evenly incorporated into the myelin structure enables recording the spectra, containing information on the structure and dynamics of lipid phase. Even though the method of ESR on the spin-labeled myelin sheath is perturbing the system by insertion of spin probe molecules, the probed environment is practically intact in all other respects, so the method applied is non-invasive and non-destructive biologically.

The spectra of the spin-labeled myelin sheath appeared to be complex (as expected for the heterogeneous lipid structure) and concomitantly were analyzed by numerical simulation using three spectral components, distinguished predominantly through different order parameters. The choice of components was made in order to meet some empirical (outer and inner hyperfine splitting) and numerical (optimization of calculated spectra) requirements. For the control spectra, spectral components I and II were defined by relatively high values of order parameters. Together with their summed relative proportions of almost 90% (Fig. 3), we could give the first estimate of the myelin lipid phase as a highly ordered structure, the result being in accordance with previous experimental findings [18]. The estimate of the myelin sheath lipid phase as a highly ordered structure could be, at least partially, explained by the lipid composition of myelin itself. Namely, a high content of cholesterol (which structurally inserts between acyl chains of phospholipids) and glycolipids (which are proposed to have weak interactions through carbohydrates) suggest an ordered structure in the plane probed by our spin probe. On the other hand, myelin proteins are suggested to interact predominantly with anionic lipids; myelin basic protein is proposed to be peripherally bound to anionic phospholipids via electrostatic interactions [19] and

proteolipids as integral proteins have strong selective affinity for anionic lipids [20]. Since cholesterol, glycolipids and anionic phospholipids represent approximately 90% of total myelin lipid content, we suggest that our spectral components I and II predominantly originate from the regions populated by these lipid classes.

The comparative analysis of results on control and diabetic samples showed that the fraction of the spectral component II is significantly increased in the spectra taken from nerve samples of diabetic rats (Figs. 2 and 3). The result suggests the increase in the number of lipid molecules situated in a less ordered environment, or in other words, an increase of the average lipid phase fluidity. The origin of such a fluidity change was tested through some simple models: (a) experimental model for demyelination (locally treated nerve fiber with EB *in vivo*), (b) proteolytic action of trypsin on the nerve fiber *in vitro*, and (c) changed osmotic conditions for the nerve fiber *in vitro*. The ESR spectral analysis of EB-treated nerves show the structural and dynamical characteristics similar to the changes seen in spectra of diabetic samples (Figs. 2 and 3). Since the EB treatment promotes ultrastructural changes of myelin sheath very similar to demyelinating change in diabetes [21], the similarity of ESR results confirms the suitability of the method applied. On the other hand, the proteolytic action of trypsin produced fluidity changes of different quality in the myelin sheath lipid phase with respect to the controls; the increased myelin sheath fluidity was expressed through significant lowering of order parameter values, with the increased relative proportion of spectral component III (Table 2), most probably being the consequence of altered lipid–protein and protein–protein interactions responsible for intralayer structuring. The changed osmotic conditions, either hyperosmotic or hypo-osmotic, produced no significant alterations in the sense of ESR simulation parameters.

In spite of the fact that this work needs additional research, let us propose a possible mechanism that could explain our results. The relative increase in proportion of spectral component II (and concomitant decrease in proportion of spectral component I) suggests lipid phase order disturbance. Although the pathological conditions of diabetes, especially hyper-

glycemia, could be the origin of such a result, the increased fluidity could be simply produced via the changed lipid composition of the myelin sheath in diabetic rats with respect to the non-pathological myelin. This hypothesis is supported by the results obtained on EB-treated nerves knowing that the EB toxicity is primarily targeted to Schwann cell metabolism. On the other hand, the proteolytic action of trypsin on non-pathological myelin produced increased fluidity, but of different quality, probably as a consequence of altered lipid–protein and/or protein–protein interactions, responsible for lipid phase structure ordering. Additional support of our hypothesis for changed myelin lipid composition in pathology of diabetes, comes from very recent and similar findings on myelin sheath isolated from galactocerebroside- and sulfatide-deficient mice nerves which are associated with severe neurological deficits [18]. Altered lipid composition was clearly correlated with changed biophysical properties (such as increased fluidity), suggesting that changes of biophysical properties of myelin sheath could indicate a common marker and the first step in development of different neuropathies. In addition, there are reports on changed human sciatic nerve phospholipid profiles in diabetes [22], so the possible change in lipid composition in case of SZT-induced diabetes in rats (already suggested from results obtained by X-ray diffraction on myelin sheath [23], would suitably explain the result of changed myelin lipid phase fluidity reported here.

Acknowledgements

This work was supported by operating Grants No. 062019 (A.S.) and 062300 (M.Z-B.) funded by Ministry of Science and Technology, Republic of Croatia.

References

- [1] Thomas, P.K. and Tomlinson, D.R. (1993) in: *Peripheral neuropathy*, B. Saunders Company, Philadelphia, PA.
- [2] A.I. Vinik, P.G. Newlon, T.J. Lauterio, F.J. Liuzzi, A.S. Depto, G.L. Pittenger, D.W. Richardson, *Diabetes Rev.* 3 (1995) 139–157.
- [3] S. Qusthoff, *Muscle Nerve* 21 (1998) 1246–1255.
- [4] A.A. Sima, M.B. Brown, A. Prashar, S. Chakrabarti, C. Laudadio, D.A. Greene, *Diabetologia* 35 (1992) 560–569.
- [5] D. Maysinger, J. Kriz, T. Hashiguchi, A.L. Padjen, *Soc. Neurosci. Abstr.* 23 (1997) 830.
- [6] J. Kriz, T. Hashiguchi, A. Tanaka, J. Mrcic, D. Maysinger, A.L. Padjen, *Can. J. Diab. Care* 21 (Suppl. 3) (1997) 63.
- [7] S. Horne, S. Quasthoff, P. Grafe, H. Bostock, R. Renner, B. Schrank, *Muscle Nerve* 19 (1996) 1268–1275.
- [8] H. Schindler, J. Seelig, *J. Chem. Phys.* 59 (1973) 1841–1850.
- [9] L.I. Horvath, P.J. Brophy, D. Marsh, *Biochemistry* 27 (1988) 5296–5304.
- [10] L.I. Horvath, P.J. Brophy, D. Marsh, *Biophys. J.* 64 (1993) 622–631.
- [11] M. Zuvic-Butorac, P. Muller, P.T. Pomorski, L. Libera, A. Herrmann, M. Schara, *Eur. Biophys. J.* 28 (1999) 302–311.
- [12] A. Laporte, H. Richard, E. Bonnaud, P. Henry, A. Vital, D. Georgescauld, *J. Neurol. Sci.* 43 (1979) 345–346.
- [13] C. Rerup, *Pharmacol. Rev.* 22 (1970) 485–517.
- [14] L. Hounson, D.R. Tomlinson, *Clin. Neurosci.* 4 (1997) 380–389.
- [15] P.K. Thomas, N.G. Beamish, J.R. Small, R.H. King, S. Tesfaye, J.D. Ward, C. Tsigos, R.J. Young, A.J. Boulton, *Acta Neuropathol.* 92 (1996) 614–620.
- [16] P.B. Jaffey, B.B. Gelman, *J. Comp. Neurol.* 373 (1996) 55–61.
- [17] A. Wright, H. Nukada, *Acta Neuropathol.* 88 (1994) 571–578.
- [18] A. Bosio, E. Binczek, W.F. Haupt, W.J. Stoffel, *J. Neurochem.* 70 (1998) 308–315.
- [19] H.M. Reinl, T.M. Bayerl, *Biochim. Biophys. Acta* 1151 (1993) 127–136.
- [20] D. Houbre, P. Schindler, E. Trifilieff, B. Luu, G. Duportail, *Biochim. Biophys. Acta* 1029 (1990) 136–142.
- [21] L.A. Pereira, M.S. Dertkigil, D.L. Graca, M.A. Cruz-Hofling, *J. Sub. Cytol. Pathol.* 30 (1998) 341–348.
- [22] D. Driscoll, W. Ennis, P. Meneses, *Int. J. Biochem.* 26 (1994) 759–767.
- [23] D.A. Kirschner, J. Eichberg, *J. Neurosci. Res.* 38 (1994) 142–148.